JOC Article

# Alkali Metal Ion Catalysis and Inhibition in Nucleophilic Displacement Reactions at Phosphorus Centers: Ethyl and Methyl Paraoxon and Ethyl and Methyl Parathion†

Ik-Hwan Um,* Young-Hee Shin, Seung-Eun Lee, Kiyull Yang,‡ and Erwin Buncel*,§

*Division of Nano Sciences and Department of Chemistry, Ewha Womans University, Seoul 120-750, Korea, Department of Chemistry Education, Gyeongsang National University, Jinju 660-701, Korea, and Department of Chemistry, Queen's University, Kingston, Ontario K7L 3N6, Canada*

*ihum@ewha.ac.kr; buncele@chem.queensu.ca*

*Received October 2, 2007*

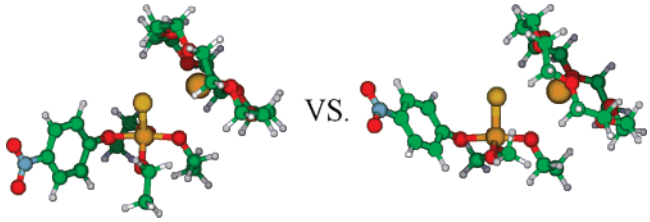


We report on the ethanolysis of the P═O and P═S compounds ethyl and methyl paraoxon (**1a** and **1b**) and ethyl and methyl parathion (**2a** and **2b**). Plots of spectrophotometrically measured rate constants, $k_{obsd}$ versus [MOEt], the alkali ethoxide concentration, show distinct upward and downward curvatures, pointing to the importance of ion-pairing phenomena and a differential reactivity of free ions and ion pairs. Three types of reactivity and selectivity patterns have been discerned: (1) For the P═O compounds **1a** and **1b**, LiOEt > NaOEt > KOEt > $EtO^-$; (2) for the P═S compound **2a**, KOEt > $EtO^-$ > NaOEt > LiOEt; (3) for P═S, **2b**, 18C6-crown-complexed KOEt > KOEt = $EtO^-$ > NaOEt > LiOEt. These selectivity patterns are characteristic of both catalysis and inhibition by alkali-metal cations depending on the nature of the electrophilic center, P═O vs P═S, and the metal cation. Ground-state (GS) vs transition-state (TS) stabilization energies shed light on the catalytic and inhibitory tendencies. The unprecedented catalytic behavior of crowned-$K^+$ for the reaction of **2b** is noteworthy. Modeling reveals an extreme steric interaction for the reaction of **2a** with crowned-$K^+$, which is responsible for the absence of catalysis in this system. Overall, P═O exhibits greater reactivity than P═S, increasing from 50- to 60-fold with free $EtO^-$ and up to 2000-fold with LiOEt, reflecting an intrinsic P═O vs P═S reactivity difference (thio effect). The origin of reactivity and selectivity differences in these systems is discussed on the basis of competing electrostatic effects and solvational requirements as function of anionic electric field strength and cation size (Eisenman's theory).

## Introduction

Phosphoryl and thiophosphoryl transfer reactions are of prime importance in biological systems. The transfer of a phosphoryl group between ATP and ADP is the fundamental mechanism for energy transfer that allows the processes of synthesis, active transport, muscle action, and nerve function to occur. Numerous studies have been reported of phosphoryl and thiophosphoryl transfer processes, both enzymically and nonenzymically.[1−10] Currently, organophosphorus (OP) derivatives are widely used as pesticides and herbicides, while they also display significant

† This paper is dedicated to Professor William (Bill) P. Jencks, a true gentleman, in acknowledgment of his immense contributions to Chemistry and Biochemistry.

‡ Gyeongsang National University.

§ Queen's University.

(1) (a) Jencks, W. P. *Catalysis in Chemistry and Enzymology*; McGraw-Hill: New York, 1969. (b) Cleland, W. W.; Hengge, A. C. *Chem. Rev.* **2006**, *106*, 3252−3278. (c) Hengge, A. C. *Adv. Phys. Org. Chem.* **2005**, *40*, 49−108. (d) Catrina, I.; O'Brien, P. J.; Purcell, J.; Nikolic-Hughes, I.; Zalatan, J. G.; Hengge, A. C.; Herschlag, D. *J. Am. Chem. Soc.* **2007**, *129*, 5760−5765. (e) Rawlings, J.; Cleland, W. W.; Hengge, A. C. *J. Am. Chem. Soc.* **2006**, *128*, 17120−17125. (f) Hengge, A. C.; Onyido, I. *Curr. Org. Chem.* **2005**, *9*, 61−74. (g) Sorensen-Stowell, K.; Hengge, A. C. *J. Org. Chem.* **2005**, *70*, 8303−8308. (h) Sorensen-Stowell, K.; Hengge, A. C. *J. Org. Chem.* **2005**, *70*, 4805−4809.

10.1021/jo702138h CCC: $40.75 
Published on Web 01/03/2008

toxicity toward mammalian organisms.[9,10] Their mode of action is on the enzyme acetylcholinesterase, involved in the transmission of nerve impulses, through phosphorylation and subsequent inactivation. Thus, paraoxon and parathion both act as nerve agents; hence, their destruction under mild conditions is an important endeavor.[6,9,10]

We have reported in a series of studies on the catalytic efficiency of alkali-metal ions on the decomposition of various OP models, including phosphinate, phosphonate, and phosphate derivatives, shown below.[7,8a] These studies have revealed different interesting selectivity patterns among the alkali-metal ions.

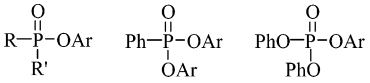

Selectivity among alkali-metal ions is a feature of a number of important biological processes, a well-known case being that of potassium and sodium ions, with high $K^+$ and low $Na^+$ concentrations maintained in mammalian cells by $Na^+-K^+$ pumps.[11]

In continuation of these works, we have examined the selectivity among alkali-metal ions of their effect on the ethanolysis of ethyl and methyl paraoxon (**1a**, **1b**) and ethyl

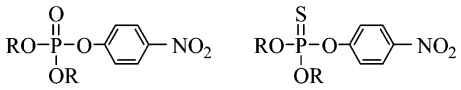

**1a**, R = Et **2a**, R = Et
**1b**, R = Me **2b**, R = Me

and methyl parathion (**2a**, **2b**). Our study has revealed an unusual range of catalysis and inhibition as well as reactivity/selectivity patterns and contrasting behaviors of the ubiquitous alkali-metal cations toward P═O and P═S systems.

## Results

The ethanolysis of ethyl and methyl paraoxon and ethyl and methyl parathion was found to proceed through P−OAr bond fission according to eq 1 with quantitative liberation of 4-nitrophenoxide ion as determined spectrophotometrically.

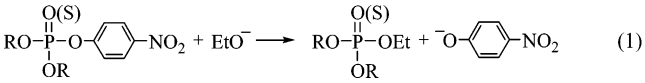

(1)

First-order kinetics was observed under the reaction conditions with MOEt (M = Li, Na, K) concentration in large excess. Pseudo-first-order rate constants ($k_{obsd}$) were obtained from plots of $\ln(A_\infty - A_t)$ vs $t$, which were linear over 90% reaction. It is estimated from replicate runs that the uncertainty in the $k_{obsd}$ values is less than ±3%. Tables S1 and S2 in Supporting Information present the $k_{obsd}$ data as a function of [MOEt] (M = Li, Na, K) for ethyl and methyl paraoxon (**1a**, **1b**) and ethyl and methyl parathion (**2a**, **2b**), respectively. The $k_{obsd}$ values as a function of [MOEt] for the reactions of **1a**, **1b**, **2a**, and **2b** are also shown in Figures 1 and 2.

## Discussion

**Curvature of Rate Plots and Its Origin.** It is immediately apparent from plots of the $k_{obsd}$ data as a function of the alkali ethoxide concentration (Figure 1) that the alcoholysis of ethyl paraoxon (**1a**) and ethyl parathion (**2a**) cannot be described as simple first order in alkali ethoxide concentration. Thus, instead

(2) (a) Onyido, I.; Swierzek, K.; Purcell, J.; Hengge, A. C. *J. Am. Chem. Soc*. **2005**, *127*, 7703−7711. (b) Sorensen-Stowell, K.; Hengge, A. C. *J. Org. Chem*. **2006**, *71*, 7180−7184. (c) Purcell, J.; Hengge, A. C. *J. Org. Chem*. **2005**, *70*, 8437−8442.

(3) (a) Tsang, J. S.; Neverov, A. A.; Brown, R. S. *J. Am. Chem. Soc.* **2003**, *125*, 7602−7607. (b) Tsang, J. S. W.; Neverov, A. A.; Brown, R. S. *J. Am. Chem. Soc.* **2003**, *125*, 1559−1566. (c) Gibson, G. T. T.; Mohamed, M. F.; Neverov, A. A.; Brown, R. S. *Inorg. Chem.* **2006**, *45*, 7891−7902. (d) Gibson, G. T. T.; Neverov, A. A.; Teng, A. C.-T.; Brown, R. S. *Can. J. Chem.* **2005**, *83*, 1268−1276. (e) Desloges, W.; Neverov, A. A.; Brown, R. S. *Inorg. Chem.* **2004**, *43*, 6752−6761. (f) Tsang, J. S. W.; Neverov, A. A.; Brown, R. S. *Org. Biomol. Chem.* **2004**, *2*, 3457−3463.

(4) (a) Terrier, F.; Le Guevel, E.; Chatrousse, A. P.; Moutiers, G.; Buncel, E. *Chem. Commun*. **2003**, 600−601. (b) Terrier, F.; Rodriguez-Dafonte, P.; Le Guevel, E.; Moutiers, G. *Org. Biomol. Chem.* **2006**, *4*, 4352−4363. (c) Moutiers, G.; Le Guevel, E.; Villien, L.; Terrier, F. *Electroanal*. **2004**, *12*, 1403−1407. (d) Terrier, F.; Moutiers, G.; Xiao, L.; Le Guevel, E.; Guir, F. *J. Org. Chem*. **1995**, *60*, 1748−1754.

(5) (a) Morales-Rojas, H.; Moss, R. A. *Chem. Rev*. **2002**, *102*, 2497. (b) Zalatan, J. G.; Herschlag, D. *J. Am. Chem. Soc*. **2006**, *128*, 1293−1303. (c) Bourne, N.; Chrystiuk, E.; Davis, A. M.; Williams, A. *J. Am. Chem. Soc*. **1988**, *110*, 1890−1895. (d) Feng, G.; Mareque-Rivas, J. C.; Williams, N. H. *Chem. Commun*. **2006**, 1845−1847. (e) Zhang, L.; Xie, D.; Xu, D.; Guo, H. *Chem. Commun*. **2007**, 1638−1640. (f) Sohn, J.; Buhrman, G.; Rudolph, J. *Biochemistry* **2007**, *46*, 807−818. (g) Stern, A. L.; Burgos, E.; Salmon, L.; Cazzulo, J. J. *Biochem. J.* **2007**, *401*, 279−285. (h) Wallace, K. J.; Fagbemi, R. I.; Folmer-Andersen, F. J.; Morey, J.; Lynth, V. M.; Anslyn, E. V. *Chem. Commun*. **2006**, 3886−3888. (i) Fanning, A.-M.; Plush, S. E.; Gunnlaugsson, T. *Chem. Commun*. **2006**, 3791−3793. (j) Klinkel, K. L.; Kiemele, L. A.; Gin, D. L.; Hagadorn, J. R. *Chem. Commun*. **2006**, 2919−2921. (k) Valeeva, F. G.; Bel'skii, V. E.; Fedorov, S. B.; Kudryavtseva, L. A.; Sakulin, G. S.; Ivanov, B. E. *Izv. Akad. Nauk SSSR, Ser. Khim*. **1988**, *12*, 2752−2756.

(6) ) (a) Han, X.; Balakrishnan, V. K.; Buncel, E. *Langmuir* **2007**, *23*, 6519−6525. (b) Han, X.; Balakrishnan, V. K.; van Loon, G. W.; Buncel, E. *Langmuir* **2006**, *22*, 9009−9017. (c) Cheung, J. C. F.; Park, Y. S.; Smith, V. H.; van Loon, G.; Buncel, E.; Churchill, D. *Can. J. Chem.* **2006**, *84*, 926. (d) Churchill, D.; Cheung, J. C. F.; Park, Y. S.; Smith, V. H.; van Loon, G.; Buncel, E. *Can. J. Chem.* **2006**, *84*, 702−708. (e) Balakrishnan, V. K.; Buncel, E.; van Loon, G. W. *Environ. Sci. Technol*. **2005**, *39*, 5824−5830. (f) Balakrishnan, V. K.; Han, X.; van Loon, G. W.; Dust, J. M.; Toullec, J.; Buncel, E. *Langmuir* **2004**, *20*, 6586−6593.

(7) (a) Pregel, M. J.; Dunn, E. J.; Nagelkerke, R.; Thatcher, G. R. J.; Buncel, E. *Chem. Soc. Rev.* **1995**, 449−455. (b) Buncel, E.; Albright, K. G.; Onyido, I. *Org. Biomol. Chem.* **2005**, *3*, 1468−1475. (c) Buncel, E.; Albright, K. G.; Onyido, I. *Org. Biomol. Chem.* **2004**, *2*, 601−610. (d) Nagelkerke, R.; Thatcher, G. R. J.; Buncel, E. *Org. Biomol. Chem*. **2003**, *1*, 163−167. (e) Buncel, E.; Nagelkerke, R.; Thatcher, G. R. J. *Can. J. Chem.* **2003**, *81*, 53−63. (f) Dunn, E. J.; Moir, R. Y.; Buncel, E. J.; Purdon, G.; Bannard, R. A. B. *Can. J. Chem.* **1990**, *68*, 1837−1845. (g) Dunn, E. J.; Buncel, E. *Can. J. Chem.* **1989**, *67*, 1440−1448.

(8) (a) Um, I. H.; Jeon, S. E.; Baek, M. H.; Park, H. R. *Chem. Commun*. **2003**, 3016−3017. (b) Um, I. H.; Hong, J. Y.; Buncel, E. *Chem. Commun*. **2001**, 27−28. (c) Um, I. H.; Akhtar, K.; Shin, Y. S.; Han, J. Y. *J. Org. Chem*. **2007**, *72*, 3823−3829. (d) Um, I. H.; Shin, Y. S.; Han, J. Y.; Mishima, M. *J. Org. Chem*. **2006**, *71*, 7715−7720.

(9) (a) Eyer, P.; Szinicz, L.; Thiermann, H.; Worek, F.; Zilker, T. *Toxicology* **2007**, *233*, 108−119. (b) Petroianu, G. A.; Arafat, K.; Nurulain, S. M.; Kuca, K.; Kassa, J. *J. Appl. Toxicol.* **2007**, *27*, 168−175. (c) Briseno-Roa, L.; Hill, J.; Notman, S.; Sellers, D.; Smith, A. P.; Timperley, C. M.; Wetherell, J.; Williams, N. H.; Williams, G. R.; Fersht, A. R.; Griffiths, A. D. *J. Med. Chem.* **2006**, *49*, 246−255. (d) Yu, S. J. *Pestic. Biochem. Phys.* **2006**, *84*, 135−142. (e) Iche-Tarrat, N.; Barthelat, J.-C.; Rinaldi, D.; Vigroux, A. *J. Phys. Chem. B.***2005**, *109*, 22570−22580. (f) Silva Filho, M. V.; Oliveira, M. M.; Salles, J. B.; Bastos, V. L. F. C.; Cassano, V. P. F.; Bastos, J. C. *Toxicol. Lett.* **2006**, *153*, 247−254. (g) Jackson, C. J.; Liu, J.-W.; Coote, M. L.; Ollis, D. L. *Org. Biomol. Chem*. **2005**, *3*, 4343−4350. (h) Wan, H. B.; Wong, M. K.; Mok, C. Y. *Pestic. Sci.* **1994**, *42*, 93−99.

(10) (a) Mishra, S.; Reddy-Noone, K.; Jain, A.; Verma, K. K. *Int. J. Environ. Pollut.* **2006**, *27*, 49−63. (b) Duquesne, S.; Reynaldi, S.; Liess, M. *Environ. Toxicol. Chem.* **2006**, *25*, 1196−1199. (c) Lartiges, S. B.; Garrigues, P. P. *Environ. Sci. Technol*. **1995**, *29*, 1246−1254. (d) Lacorte, S.; Barcelo-, D. *Environ. Sci. Technol.* **1994**, *28*, 1159−1163.

(11) Nelson, D. L.; Cox, M. M. *Lehninger Principles of Biochemistry*, 4th ed.; W. H. Freeman and Co.: New York, 2004; pp 409−428.

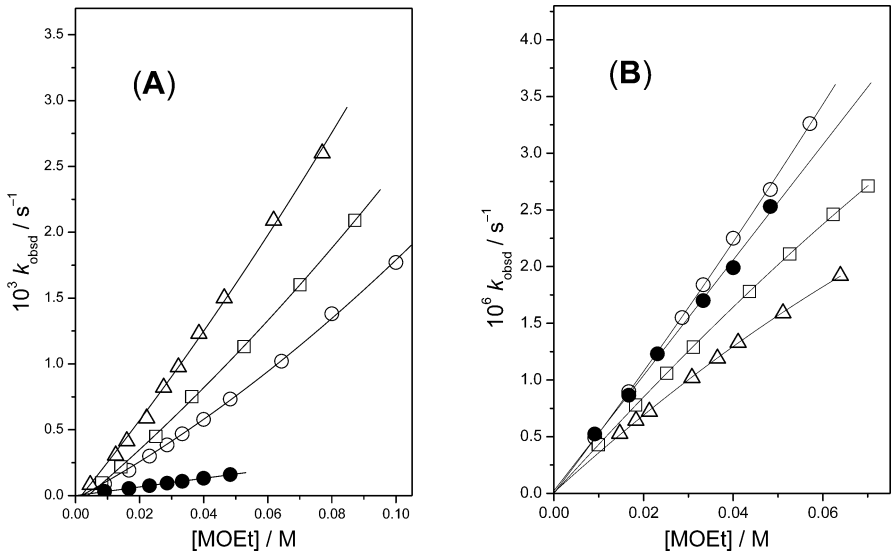


**FIGURE 1.** Plots of $k_{obsd}$ vs [MOEt] for the reactions of ethyl paraoxon, **1a** (A) and ethyl parathion, **2a** (B) with LiOEt (△), NaOEt (□), KOEt (○), and KOEt in the presence of 18C6 (● [18C6]/[KOEt] = 5.0) in anhydrous EtOH at 25.0 ± 0.1 °C.

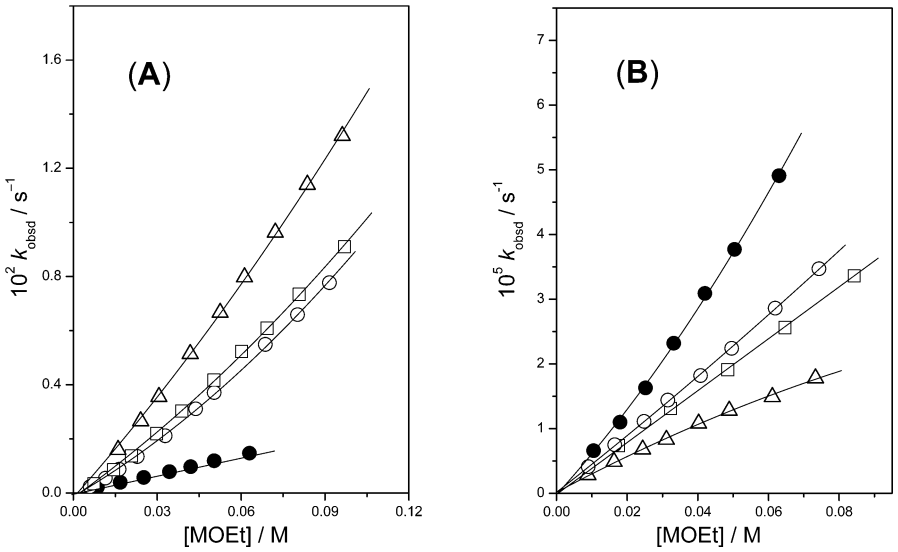


**FIGURE 2.** Plots of $k_{obsd}$ vs [MOEt] for the reactions of methyl paraoxon, **1b** (A) and methyl parathion, **2b** (B) with LiOEt (△), NaOEt (□), KOEt (○), and KOEt in the presence of 18C6 (● [18C6]/[KOEt] = 5.0) in anhydrous EtOH at 25.0 ± 0.1 °C.

of linear $k_{obsd}$ vs [MOEt] plots, Figure 1 reveals both upward- and downward-curved plots.

On the other hand, addition of 18-crown-6 ether (18C6) to the ethyl paraoxon/KOEt solution results in linear plots, suggesting that reactivity in these systems is determined at the origin by ion-pairing. Accordingly, the reactivity order revealed for ethyl paraoxon (Figure 1A), i.e., LiOEt > NaOEt > KOEt >KOEt/crown, imparts the greatest catalytic efficiency to the LiOEt ion pair. Note that, contrastingly, in systems where ion-pairing impedes reaction, the reverse order, i.e., KOEt > NaOEt > LiOEt, prevails.[12]

Proceeding to the reaction of ethyl parathion (**2a**), an interesting contrast becomes apparent compared to ethyl paraoxon described above. Thus, the selectivity order revealed in Figure 1B, $K^+ > Na^+ > Li^+$, is the opposite of that seen for ethyl paraoxon in Figure 1A. Note also that introduction of 18C6 imparts a different reactivity pattern in Figure 1B compared to Figure 1A. This finding of higher reactivity of crowned-$K^+$ is quite unusual in studies with other organophosphorus derivatives[7] and will be considered further subsequently.

The plots for methyl paraoxon (**1b**) and methyl parathion (**2b**), in Figure 2A,B, exhibit similar behavior as for the ethyl analogs in Figure 1A,B, except that crowned-$K^+$ has higher reactivity compared to $K^+$ alone. This will also receive scrutiny subsequently.

**Dissection of $k_{obsd}$ into Free and Ion-Paired Alkali Ethoxide Reactivities: P=O vs P=S.** As indicated above, the curvature observed in the $k_{obsd}$ vs [MOEt] rate plots is indicative of a prevailing ion-pairing phenomenon and a differential reactivity of free ions and ion pairs. In the region of alkali ethoxide concentration below 0.1 M, as in the present study, one can exclude dimers and other aggregates from being present. Hence, the rate law in eq 2 which assigns different reactivities to free ions and ion pairs will hold with $k_{obsd}$ expressed by eq

(12) Jones, J. R. *Prog. React. Kinet.* **1973**, *7*, 1−22.

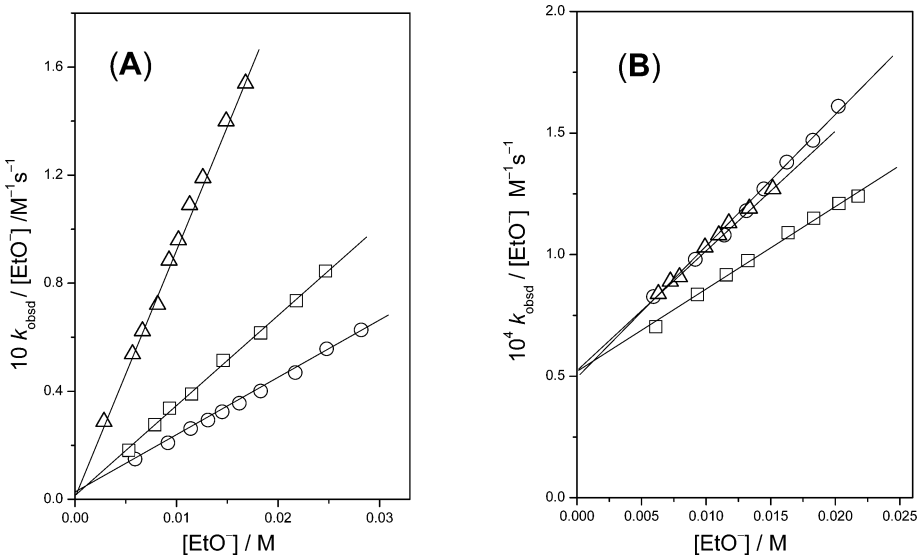


**FIGURE 3.** Plots of $k_{obsd}/[EtO^-]_{eq}$ vs $[EtO^-]_{eq}$ for reactions of ethyl paraoxon, **1a** (A) and ethyl parathion, **2a** (B) with LiOEt (△), NaOEt (□), and KOEt (○) in anhydrous EtOH at 25.0 ± 0.1 °C.

**TABLE 1. Summary of Second-Order Rate Constants for Various Ethoxide Species from Ion-Pairing Treatment of Kinetic Data for the Reaction of Ethyl Paraoxon (1a) and Ethyl Parathion (2a) with MOEt in Anhydrous EtOH at 25.0 ± 0.1 °C**

| | $10^5$ $k_{EtO^-}$/M$^{-1}$ s$^{-1}$ | | $10^5$ $k_{MOEt}$/M$^{-1}$ s$^{-1}$ | |
|---|---|---|---|---|
| | **1a** | **2a** | **1a** | **2a** |
| LiOEt | – | – | 4350 | 2.34 |
| NaOEt | – | – | 3250 | 3.40 |
| KOEt | 329[a] | 5.06[b] | 2400 | 6.11 |

[a] Obtained from the slope of $k_{obsd}$ vs [KOEt] plot in the presence of 18C6. [b] An average value for all alkali metals.

**TABLE 2. Summary of Second-Order Rate Constants for Various Ethoxide Species from Ion-Pairing Treatment of Kinetic Data for the Reaction of Methyl Paraoxon (1b) and Methyl Parathion (2b) with MOEt in Anhydrous EtOH at 25.0 ± 0.1 °C**

| | $10^4$ $k_{EtO^-}$/M$^{-1}$ s$^{-1}$ | | $10^4$ $k_{MOEt}$/M$^{-1}$ s$^{-1}$ | |
|---|---|---|---|---|
| MOEt | **1b** | **2b** | **1b** | **2b** |
| LiOEt | – | – | 1710 | 1.83 |
| NaOEt | – | – | 1270 | 3.78 |
| KOEt | 233[a] | 4.69[b] | 1180 | 4.69 |

[a] Obtained from the slope of $k_{obsd}$ vs [KOEt] plot in the presence of 18C6. [b] Determined through nonlinear least-squares fitting of eq 3.

3. Equation 3 can be transformed into eq 4, and from the known association constant $K_a$ (i.e., $K_a = [MOEt]/[M^+][EtO^-]$, $K_a$ = 212, 102, and 90 M$^{-1}$ for LiOEt, NaOEt, and KOEt, in turn),[13] one can calculate $k_{EtO^-}$ and $k_{MOEt}$

$$\text{rate} = k_{EtO^-}[EtO^-][\mathbf{1} \text{ or } \mathbf{2}] + k_{MOEt}[MOEt][\mathbf{1} \text{ or } \mathbf{2}] \quad (2)$$

$$k_{obsd} = k_{EtO^-}[EtO^-] + k_{MOEt}[MOEt] \quad (3)$$

$$k_{obsd}/[EtO^-] = k_{EtO^-} + K_a k_{MOEt}\,[EtO^-] \quad (4)$$

Plots of $k_{obsd}/[EtO^-]$ vs $[EtO^-]$ for ethyl paraoxon and ethyl parathion (Figure 3A,B) are linear, the slope of each line yielding $k_{MOEt}$ using the known values of $K_a$ for each alkali ethoxide.[13] While the small intercept in Figure 3A does not allow a reliable value of $k_{EtO^-}$ to be deduced, this is obtained from the slope of the $k_{obsd}$ vs $[EtO^-]$ plot in the presence of 18C6 in Figure 1A. The resulting $k_{obsd}$ and $k_{MOEt}$ values for ethyl paraoxon (**1a**) and ethyl parathion (**2a**) are given in Table 1, while corresponding data for methyl paraoxon (**1b**) and methyl parathion (**2b**) are presented in Table 2.

The following trends in reactivity and selectivity patterns can be seen in Tables 1 and 2, following dissection of the rate data according to Tables 1 and 2.

(1) Modification of the electrophilic center from P═O (**1a**, **1b**) to P═S (**2a**, **2b**) and including the crowned-K$^+$ data results in a 50−60-fold decrease in reactivity toward dissociated EtO$^-$. This is a further example of an intrinsic P═O vs P═S reactivity, also known as the thio effect.[2,8c,8d,14] This reactivity order is similar to previous reports on reactivities of other P═O and P═S derivatives toward nucleophiles (e.g., OH$^-$, ArO$^-$, and amines).[2,8c,8d,14]

(2) Perhaps the most striking observation that follows from the present results, displayed in Figures 1 and 2, is the lack of consistency in selectivity order. On the one hand, we see the alkali-metal catalytic efficacy toward **1a** and **1b** (P═O), LiOEt > NaOEt > KOEt > EtO$^-$, the previously observed selectivity order in the phosphinate series.[7] On the other hand, **2a** (P═S) shows the selectivity order KOEt > EtO$^-$ > NaOEt > LiOEt, while for **2b** (P═S) one sees KOEt/crown > KOEt = EtO$^-$ > NaOEt > LiOEt.

Note that the thio effect becomes greatly magnified when one considers P═O versus P═S reactivity by the MOEt series rather than by EtO$^-$. In fact, since the P═O/LiOEt reaction

(13) Barthel, J.; Justice, J-C.; Wachter, R. *Z. Phys. Chem.* **1973**, *84*, 100−113.

(14) (a) Morles-Rojas, H.; Moss, R. A. *Chem. Rev.* **2002**, *102*, 2497−2521. (b) Yang, Y. C.; Baker, J. A.; Ward, J. R. *Chem. Rev.* **1992**, *92*, 1729−1743. (c) Quin, L. D. *A Guide to Organophosphorus Chemistry*; Wiley: New York, 2000. (d) Wu, T. G.; Qiu, J. U. *Environ. Sci. Technol.* **2006**, *40*, 5428−5434. (e) Eyer, P. *Toxicol. Rev.* **2003**, *22*, 165−190. (f) Kevill, D. N.; Carver, J. S. *Org. Biomol. Chem.* **2004**, *2*, 2040−2043. (g) Kevill, D. N.; D'Souza, M. J. *Can. J. Chem.* **1999**, *77*, 1118. (h) Kevill, D. N.; Bond, M. W.; D'Souza, M. J. *J. Org. Chem.* **1997**, *62*, 7869.(i) Kevill, D. N.; D'Souza, M. J. *J. Chem. Soc., Perkin Trans. 2* **1997**, 1721. (j) Herschlag, D.; Piccirilli, J. A.; Cech, T. R. *Biochemistry* **1991**, *30*, 4844−4854.

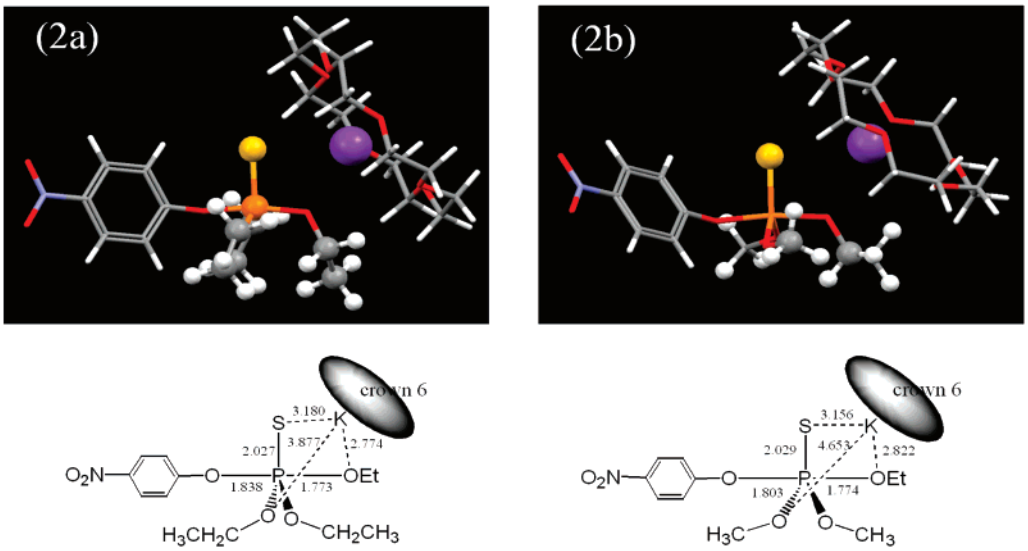


**FIGURE 4.** The geometrically optimized structures of the intermediates for the reaction of ethyl parathion (**2a**) and methyl parathion (**2b**) with KOEt in the presence of 18C6, showing three crowded ethoxy groups for the reaction of **2a**, contrasting with **2b**.

exhibits catalysis while the P═S/LiOEt reaction exhibits inhibition, the overall effect is magnified to a thio effect of ca. 1000−2000.

**The Unprecedented Reactivity of Crowned-KOEt.** The observation that KOEt/crown is more reactive than KOEt itself is to our knowledge unprecedented. Importantly, the KOEt/crown plot for **2b** shows upward curvature (Figure 2B) according to the catalytic reactivity to this species. In contrast, the KOEt/crown plot for **2a** (Figure 1B) is linear and falls below the KOEt plot. This contrasting behavior is clearly due to steric interaction between the incoming $EtO^-$ associated with the crowned-$K^+$ and the EtO groups on the central P atom. This is clearly illustrated in the energy-optimized intermediate structures for **2a** and **2b** in Figure 4, noting also that these energies differ only slightly from the transition structure. In terms of the hard and soft acids and bases (HSAB) principle,[15] the crowned-$K^+$ is viewed as a soft Lewis acid that will interact favorably with the soft P═S Lewis base. Lehn has suggested that the crown-complexed cation is accessible from above and below the plane of the crown ether in $M^+$−crown ether complexes.[16] Accordingly, weak ion-pairing of $EtO^-$ ion to the 18C6-complexed $K^+$ ion would be possible.

**Alkali Metal Catalysis and Inhibition: Paraoxon versus Parathion.** In our previous studies of the alcoholysis of a series of aryl diphenylphosphinates and aryl benzenesulfonates, it was found that the phosphinate reactions were subject to catalysis by alkali-metal cations with a selectivity order LiOEt > NaOEt > KOEt > $EtO^-$.[7] However, the benzenesulfonate reactions revealed catalysis by NaOEt and KOEt but inhibition by LiOEt.[7] It is evident that the present systems, paraoxon (**1**, P═O) and parathion (**2**, P═S), exhibit a parallel behavior to that described above, alkali metal catalysis being observed with paraoxon (Figures 1A and 2A), but inhibition with parathion (Figures 1B and 2B).

**GS and TS Interaction of $M^+$.** Generally, one can express catalysis and inhibition in these systems by Figure 5, which is reminiscent of enzymic reactions.[17] In both types of processes,

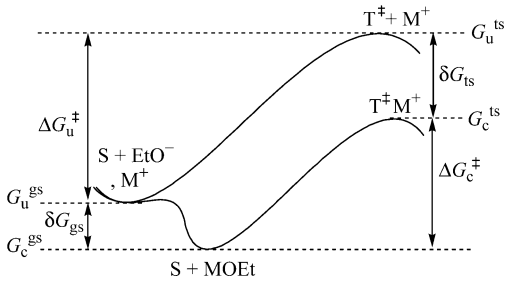


**FIGURE 5.** Free energies involved in the uncatalyzed and metal ion catalyzed reactions of an ester, S, with alkali metal ethoxide, MOEt. $\Delta G_u^{‡}$ and $\Delta G_c^{‡}$ are the activation energies for the uncatalyzed and catalyzed reactions, respectively, while $\delta G_{gs}$ and $\delta G_{ts}$ refer respectively to stabilization of GS and TS by $M^+$.

the reaction pathway follows initial complex formation by the substrate, followed by formation of the rate-determining transition state and product formation. The relative magnitude of the ground-state stabilization term, $\delta G_{gs}$, and of the transition-state stabilization term, $\delta G_{ts}$ determines the outcome, catalysis, and inhibition. Thus, $\delta G_{ts} > \delta G_{gs}$ corresponds to catalysis and $\delta G_{gs} > \delta G_{ts}$ to inhibition.

To explore the possibility of complexation of $M^+$ with **1a** and **1b** in the GS, $^{31}P$ NMR spectra of **1a** and **1b** have been taken in the absence and presence of $Li^+$ in deuteriated ethanol. $Li^+$ was expected to exert the strongest interaction with P═O, since this exhibits the most pronounced upward curvature and is most highly reactive in the $k_{obsd}$ vs [MOEt] plot. Now, one can anticipate that preassociation of $Li^+$ with P═O in **1a** and **1b** would result in an upfield shift in the $^{31}P$ NMR spectra.[18] However, in fact, the chemical shifts for **1a** and **1b** in the presence of excess $Li^+$ were identical to those in the absence of $Li^+$, indicating that complexation of $M^+$ with **1a** and **1b** does not occur in the GS, or that it is undetectably weak.

(15) Pearson, R. G.; Songstad, J. *J. Am. Chem. Soc.* **1967**, *89*, 1827.
(16) Lehn, J. M. *Pure Appl. Chem.* **1980**, *52*, 2303−2319.
(17) Gandour, R. D.; Schowen, R. L. *Transition States of Biochemical Processes*; Plenum Press: New York, 1978.
(18) (a) Ruiz-Morales, Y.; Zigler, T. *J. Phys. Chem. A* **1998**, *102*, 3970−3976. (b) Gauss, J.; Stanton, J. F. *J. Chem. Phys.* **1995**, *102*, 251−253. (c) Pehkonen, S. O.; Judeh, Z. M. A. *Environ. Sci. Technol.* **2005**, *39*, 2586−2591.

**SCHEME 1**

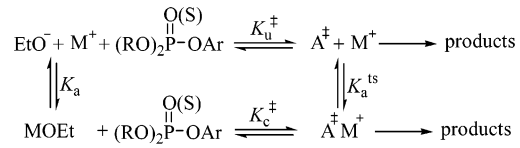

**TABLE 3. Free Energies of Stabilization of Ground State ($\delta G_{gs}$), Transition State ($\delta G_{ts}$), and the Net Catalytic Effect ($\Delta G_{cat}$) for the Reactions of 1a, 1b, 2a, and 2b with MOEt in Anhydrous EtOH at 25.0 ± 0.1 °C (all values are in kcal mol$^{-1}$)**

| metal ion | | 1a | | 1b | | 2a | | 2b | |
|---|---|---|---|---|---|---|---|---|---|
| | $\delta G_{gs}$ | $\delta G_{ts}$ | $\Delta G_{cat}$ | $\delta G_{ts}$ | $\Delta G_{cat}$ | $\delta G_{ts}$ | $\Delta G_{cat}$ | $\delta G_{ts}$ | $\Delta G_{cat}$ |
| $Li^+$ | −3.16 | −4.69 | −1.53 | −4.34 | −1.18 | −2.71 | 0.45 | −2.63 | 0.53 |
| $Na^+$ | −2.73 | −4.09 | −1.36 | −3.73 | −1.00 | −2.50 | 0.23 | −2.62 | 0.11 |
| $K^+$ | −2.66 | −3.83 | −1.17 | −3.61 | −0.95 | −2.78 | −0.12 | −2.69 | −0.03 |

This leaves us to examine stabilization of the GS through ion-pairing between $M^+$ and $EtO^-$. Differential stabilization of TS and GS can then be evaluated using a method developed by Kurz[19] and in different forms by Mandolini[20] and Tee.[21] Scheme 1 describes a set of equilibria among the reactants and TS's for the catalyzed and uncatalyzed pathways. In this thermodynamic cycle, $K_u^{\ddagger}$ and $K_c^{\ddagger}$ represent the equilibrium constants for formation of the uncatalyzed and catalyzed TS's, while $K_a$ and $K_a^{ts}$ are the association constants for ion-pairing of $M^+$ with $EtO^-$ and the TS, respectively. $K_a^{ts}$ can be calculated from the relationship $K_a^{ts} = K_a k_{MOEt}/k_{EtO^-}$ together with the reported $K_a$ values and the respective rate constants.[19] $K_a$ and $K_a^{ts}$ can also be expressed in terms of free energies of stabilization by metal ion, i.e., $\delta G_{gs}$ and $\delta G_{ts}$, respectively.

The relationship between GS and TS stabilization is illustrated in Figure 5. It is apparent that the net catalytic effect, $\Delta G_{cat}$ can be calculated from the difference in free energies of activation between the catalyzed and uncatalyzed reactions, i.e., $\Delta G_{cat} = \Delta G_c^{\ddagger} - \Delta G_u^{\ddagger} = \delta G_{ts} - \delta G_{gs}$. Accordingly, a negative $\Delta G_{cat}$ value indicates that the TS is more stabilized than the GS, and $M^+$ acts as a catalyst, while a positive $\Delta G_{cat}$ value implies that the reaction is inhibited by $M^+$. The $\delta G_{gs}$, $\delta G_{ts}$, and $\Delta G_{cat}$ values determined in the current reactions are summarized in Table 3. The magnitude of these terms is of some interest.

Table 3 shows that $\Delta G_{cat}$ values for reactions of the P═O compounds (**1a** and **1b**) are negative in all cases, indicating that here $M^+$ ions act as catalysts. Besides, the $\Delta G_{cat}$ value becomes more negative as the size of $M^+$ decreases, which is in accord with the catalytic effect for the reactions of P═O compounds (**1a** and **1b**) increasing with decreasing size of $M^+$. In contrast, for the reactions of the P═S compounds (**2a** and **2b**) with LiOEt and NaOEt, the $\Delta G_{cat}$ values are positive, indicating that $Li^+$ and $Na^+$ act as inhibitors, while $K^+$ has slight or negligible catalytic effect. This result is consistent with the preceding observation that ion-paired LiOEt and NaOEt are less reactive than dissociated $EtO^-$ toward **2a** and **2b**, exhibiting downward curvature in Figures 1B and 2B while the plots for KOEt are linear.

**TS and Reaction Intermediate Structures for Catalyzed and Uncatalyzed Reactions.** Nucleophilic substitution reactions at phosphorus centers are commonly represented either as concerted processes, $S_N2(P)$, or as proceeding by a stepwise addition−elimination mechanism, though in special cases an $S_N1(P)$-type (metaphosphate) mechanism has also been put forward (see refs 1, 2, and 5−9 for detailed discussion in the phosphinate and phosphate series). In the context of the present study, it will be assumed that the nucleophilic reactions proceed by the two-step mechanism, the first step, addition of nucleophile to P, being rate-determining.

Considering interactions with $M^+$, one possible catalytic role for metal ions could be through coordination with the oxygen center of the aryloxy group. No evidence for such a process has been found in the present work; on the contrary, if this did occur, it would be difficult to account for the contrasting metal ion effect between the P═O and P═S structures.

The most plausible explanation of metal ion catalysis in the present systems is one involving coordination to P═O and P═S, any difference (i.e., reactivity and selectivity) between the two systems being ascribed to factors such as HSAB consideration, p-orbital overlap, electronegativity, solvation, and so on. Thus, in the case of P═O compounds, electrostatic interactions would be greatest with small-sized cations. With P═S compounds, however, the dominant effect derives from their "soft" character, in accordance with the HSAB principle.

Metal ion involvement can most readily be explained on the basis of a four-membered transition state with simultaneous attack by $EtO^-$ at P and $M^+$ attachment to P═O(S) as shown below.

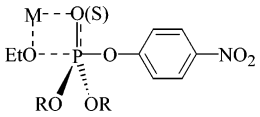

The optimized structures of the intermediates for reactions of **2a** and **2b** in the absence and presence of $K^+$ are illustrated in Figures 6 and 7, respectively. A four-membered cyclic intermediate in the presence of $K^+$ is shown in Figure 7.

**The High/Low Field Strength Model: Electrostatic vs Solvational Energy Preferences.** An alternative approach (to HSAB) that would explain the contrasting selectivity patterns toward alkali-metal cations in the P═O and P═S series is based on Eisenman's theory of ion exchange selectivity patterns being determined by competition between electrostatic factors and solvational energies.[22] Thus, according to this theory, the strength of the interaction between a cation and a fixed anionic group is determined by two competing factors: (i) electrostatic interactions resulting from the approach of ions of opposite charge and (ii) the difference in the solvation energies of the ions, accounted for by the energy required to rearrange the solvent molecules around the ions so that close contact can occur. The net standard free energy change ($\Delta G^{\circ}_{1/2}$) for the interchange of cations 1 and 2 at a fixed anionic site is the difference between the terms for electrostatic interactions and solvent rearrangement in eq 5, in which $e$ is the electronic charge, $r_1$, $r_2$, and $r_A$ are the radii of cations 1 and 2 and of the anion, respectively, and $\Delta G_1$ and $\Delta G_2$ are the solvation energies of cations 1 and 2.

$$\Delta G^{\circ}_{1/2} = \{[e^2/(r_A + r_2)] - [e^2/(r_A + r_1)] - (\Delta G_2 - \Delta G_1)\} \quad (5)$$

From eq 5, it can be predicted that for a high electric field strength, i.e., in the present system, an anionic group with

(19) Kurz, J. L. *J. Am. Chem. Soc.* **1963**, *85*, 987.
(20) Cacciapaglia, R.; Mandolini, L. *Chem. Soc. Rev.* **1993**, *22*, 221.
(21) Tee, O. S. *Adv. Phys. Org. Chem.* **1994**, *29*, 1.

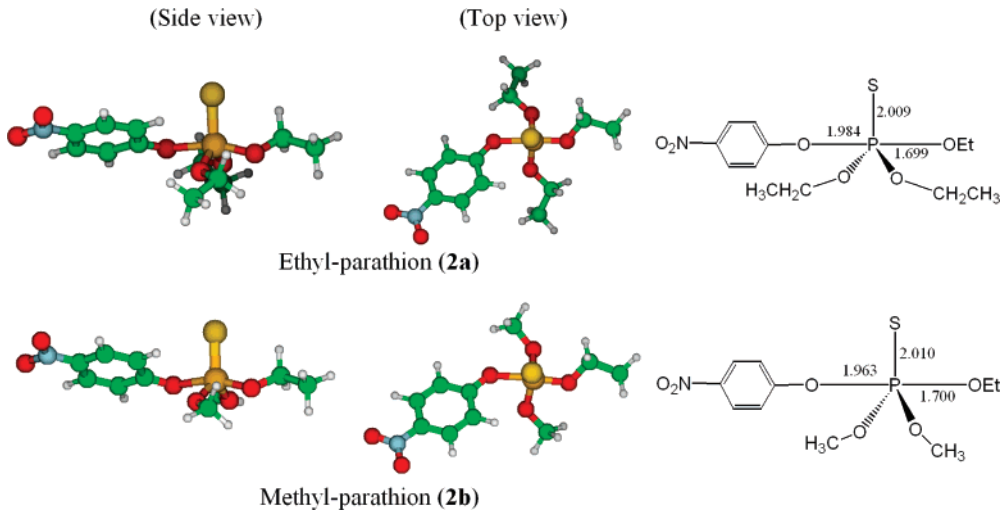


**FIGURE 6.** The structures of intermediates for reactions of **2a** and **2b** with $EtO^-$ (absence of $K^+$ ion).

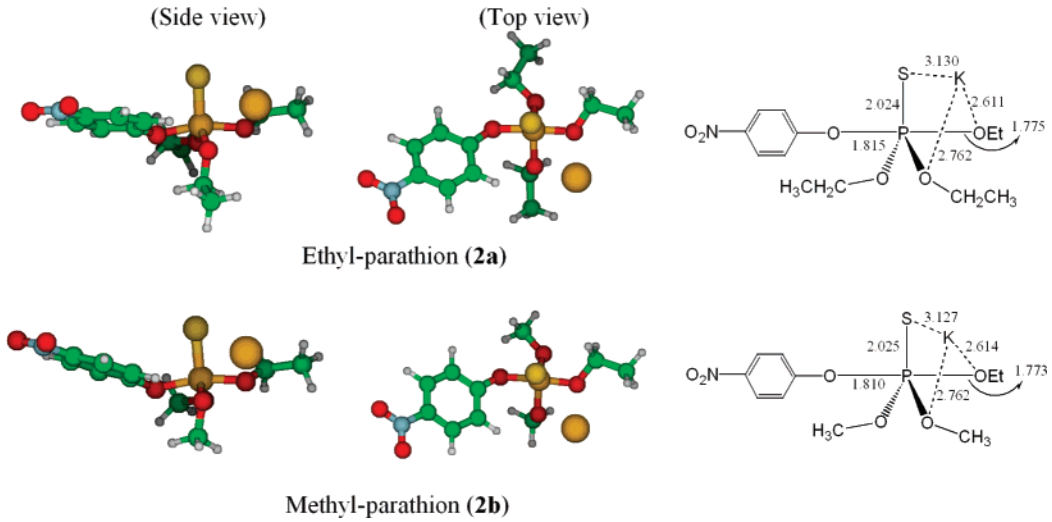


**FIGURE 7.** The structures of intermediates for reactions of **2a** and **2b** with KOEt.

**SCHEME 2**

| Substrate | Selectivity | TS | Intermediate |
|---|---|---|---|
| P=S (**2a**) | $K^+ > Na^+ > Li^+$ | $P{=}S^{\delta-}$ | $P{-}S^-$ |
| P=S (**2b**) | crowned-$K^+ > Na^+ > Li^+$ | increasing anionic electric field strength | |
| P=O (**1a**) | $Li^+ > Na^+ > K^+$ | $P{=}O^{\delta-}$ | $P{-}O^-$ |
| P=O (**1b**) | | | |

localized charge, P═O, the electrostatic term would dominate over the solvation energy term, allowing ions with opposite charge to come into direct contact. This means that for such situations, smaller ions will bind more strongly, and vice versa, resulting in the selectivity order $Li^+ > Na^+ > K^+$. These relationships are illustrated in Scheme 2.

On the other hand, when the counterion has low electric field strength, as in the P═S system, where the developing negative charge is dispersed on the polarizable S atom, it can be predicted that the solvation energy term in eq 5 would dominate over the term for electrostatic interaction. Under these conditions, the resulting selectivity order, $K^+ > Na^+ > Li^+$, is opposite to that observed in the P═O system and $\delta G_{ts}$ ($M^+$) correlates with the solvated radius of the metal ion.

## Conclusions

Studies of the ethanolysis of the P═O and P═S compounds ethyl and methyl paraoxon (**1a** and **1b**) and ethyl and methyl parathion (**2a** and **2b**) have revealed contrasting reactivity/selectivity patterns indicative of both catalysis and inhibition by alkali-metal cations. The following conclusions can be drawn.

(1) The ion-paired alkali metal ethoxides (MOEt) catalyze the reactions of **1a** and **1b** and the catalytic effect increases with decreasing size of $M^+$.

(2) The P═O compounds (**1a**, **1b**) are ca. 50−60 times more reactive than their thio analogues (**2a**, **2b**) toward dissociated $EtO^-$, which represents the intrinsic reactivity difference between the P═O and P═S compounds. However, toward LiOEt, P═O reactivity exceeds P═S reactivity up to ca. $2 \times 10^3$-fold.

(3) A four-membered cyclic TS has been proposed to account for the $M^+$ effect, in which $M^+$ increases the electrophilicity of the P-electrophilic site toward $EtO^-$.

(4) 18C6-crowned-$K^+$ forms a weak ion pair with $EtO^-$; the ion-paired species catalyzes the reaction of **2b** but not that of

(22) Eisenman, G. *Biophys. J.* **1962**, *2*, 259−323.

**2a**. The catalytic behavior of crowned-$K^+$ in the reaction with **2b** is unprecedented.

(5) Modeling studies of the pentacoordinate intermediate reveal a severe steric interaction between the incoming crowned-$K^+$ and the OEt groups, resulting in the absence of a catalytic effect for the reaction of **2a**.

(6) Two competing effects (i.e., electrostatic interaction between the two opposite charges and solvational energies required to rearrange the solvent molecules around cations) are responsible for the contrasting reactivity and selectivity patterns found in this system.

## Experimental Section

**Materials.** Compounds **1a**, **1b**, **2a**, and **2b** were of the highest quality available. The solutions of MOEt were prepared by dissolving the respective alkali metal in anhydrous ethanol under $N_2$ and stored in the refrigerator. The concentrations of MOEt were determined by titration with standard HCl solution. 18-Crown-6-ether was recrystallized from acetonitrile and dried over $P_2O_5$ in vacuo. The anhydrous ethanol used was further dried over magnesium and distilled under $N_2$.

**Kinetics.** Kinetic study was performed using a UV−vis spectrophotometer equipped with a constant-temperature circulating bath. The reactions were followed by monitoring the appearance of 4-nitrophenoxide ion at 400 nm. Pseudo-first-order conditions with MOEt at least 20 times greater than substrate concentration were used. Generally, reactions were followed for 9−10 half-lives and $k_{obsd}$ values were calculated using the equation $\ln(A_\infty - A_t)$ vs $t$. The conditions and the $k_{obsd}$ values are summarized in Tables S1−S3 in the Supporting Information.

**Product Analysis.** 4-Nitrophenoxide ion was liberated quantitatively and identified as one of the products by comparison of the UV−vis spectra under the same kinetic conditions. The $^{31}P$ NMR spectrum of the reaction mixture showed only one peak for the phosphate (or thiophosphate), indicating that the reaction proceeds only through P−OAr bond fission and no $S_N2$ reaction occurs at the $CH_3$ moiety of **1b** and **2b**.

**Calculations and Modeling of Intermediate**. The model reactions included in the quantum chemical calculations are noncatalyzed, $K^+$-catalyzed, and 18C6-complexed $K^+$-catalyzed reactions in the gas phase. All the calculations have been carried out with the Gaussian 98 package.[23] The reactants, intermediate, and the TS have been fully optimized at the density functional theory (DFT) of Becke's three-parameter hybrid method using the correlation functional of Lee et al. (B3LYP)[24] at the 6-31G(d) level. One set of diffuse functions is used for a better representation of sulfur atom (631G(d)). The TS for the reaction of **2b** with $EtO^-$ in the absence of $K^+$ ion was located by the Berny optimization algorithm using the "Opt=CalcAll" option.[25] The energy barrier between the TS and the pentavalent intermediate has been calculated to be only 0.5 kcal/mol. Accordingly, the structures of the TS and the intermediate are almost the same, except the bond length between the P and the O atom in the leaving 4-nitrophenoxide moiety (i.e., the bond lengths in the TS and intermediate are 2.23 and 1.96 Å, respectively). Accordingly, only intermediates have been calculated for the remaining reactions in view of the difficulties in locating the TS's on the almost flat potential energy surface for the large molecular systems including the crown-ether.

**Acknowledgment.** This work was supported by Korea Research Foundation (2005-015-C00256). Grateful acknowledgment is also due to the Natural Sciences and Engineering Research Council of Canada (NSERC) for research support (E.B.).

**Supporting Information Available:** $^{31}P$ NMR spectra for compounds **1a** and **1b** in the absence and the presence of $LiClO_4$ in deuterated ethanol, $^{31}P$ NMR spectra for the product of the reactions of **1b** with LiOEt and KOEt in deuterated ethanol, Tables S1−S3 for the kinetic conditions and data, complete ref 23, and optimized final coordinates S1−S4 as Gaussian 98 program input format with basis sets and electronic energy. This material is available free of charge via the Internet at http://pubs.acs.org.

JO702138H

(23) Frisch, M. J.; et al. *Gaussian 98*, Revision A.7.; Gaussian, Inc.: Pittsburgh, PA, 1998. Complete ref 23 is shown in the Supporting Information.

(24) (a) Becke, A. D. *J. Chem. Phys*. **1933**, *98*, 5648. (b) Lee, C.; Yang, W.; Parr, R. G. *Phys. Rev. B* **1988**, *37*, 785.

(25) (a) Peng, C.; Ayala, P. Y.; Schlegel, H. B.; Frisch, M. J. *J. Comp. Chem.* **1996**, *17*, 49. (b) Schlegel, H. B. *Theor. Chim. Acta* **1984**, *66*, 33.